

## Post-tsunami oceanographic conditions in southern Arabian Sea and Bay of Bengal

N. Anilkumar<sup>1,\*</sup>, Y. V. B. Sarma<sup>2</sup>, K. N. Babu<sup>1</sup>, M. Sudhakar<sup>1</sup> and P. C. Pandey<sup>1</sup>

<sup>1</sup>National Centre for Antarctic and Ocean Research, Headland Sada, Goa 403 804, India

<sup>2</sup>National Institute of Oceanography, Dona Paula, Goa 403 004, India

**Physical oceanographic conditions along the east and west coasts of India immediately after the recent devastating tsunami are presented here. The thermocline in the southeast coast exhibited trivial downward tilt towards north. A mixed layer deepening (> 50 m) associated with low-salinity (< 34 psu) and relatively colder water is noticed in the Gulf of Mannar region and along east coast of India. The low-salinity waters observed are apparently from the Bay of Bengal, driven along the coast into the Arabian Sea by north equatorial current between equator and 10°N, and the southward-flowing east India coastal current. A high-salinity tongue (> 36.0 psu) was identified as the Arabian Sea high salinity water mass along the west coast of India around 100 m depth up to 10°N. The heat content changes closely followed similar changes in the depth of the 20°C isotherm. Turbidity measurements using light scattering sensor showed the existence of two layers of high-scattering, one around 40 m and the other around 250 m. The shallow high-scattering layer is associated with high chlorophyll *a* concentration, but the deeper high-scattering layer noticed at shallow stations off the west and east coasts of India may be due to the resuspension of the sea-floor sediments due to turbulence generated by the tsunami.**

**Keywords:** Arabian Sea, Bay of Bengal, Oceanographic conditions, tsunami.

THE recent earthquake originated in the Indian Ocean just north of Simeulue island, off the western coast of northern Sumatra, Indonesia has produced the largest trans-oceanic tsunami in over 40 years and killed more people than any tsunami in recorded history. It occurred at 3.30°N, 95.8°E during 00.58 h (UTC) on 26 December 2004. The resulting tsunami devastated the shores of Indonesia, Sri Lanka, southern parts of India, Andaman and Nicobar Islands, Thailand and other countries in this region, with waves up to 15 m (50 ft) high, even reaching the east coast of Africa, 4500 km (2800 miles) west of the epicentre. At some places the waves reached as far as 2 km inland. Several tide records from along the Indian coast have also shown abrupt rise in sea level with large-amplitude waves coinciding with the arrival of the tsunami. In this back-

ground, we have conducted an oceanographic cruise on-board *ORV Sagar Kanya* to investigate the effect of tsunami on the ocean environment.

Several earlier studies<sup>1–11</sup> have described the coastal currents and upwelling features in the study area in relation to the southwest and northeast monsoons. However, these studies deal with more open ocean water characteristics than the present study. Circulation along the Indian coastal region is regulated by the southwest monsoon and northeast monsoon winds and coastal currents<sup>1,2,9</sup>. However, there is not much information available on the oceanographic conditions in the inner-shelf region (coastward from 500 m isobath) during December–January. The present dataset is the only one of its kind to investigate the influence of the tsunami on the hydrography of this region. Here we present the physical oceanographic conditions observed coastward of the 500 m isobath immediately after the tsunami event in this region.

Hydrographic data were collected from Goa to Chennai along the coastal regions of peninsular India and the Gulf of Mannar from 3 to 15 January 2005 on-board *ORV Sagar Kanya* (Figure 1). A SBE 9/11 Plus CTD fitted with rosette water sampler, light scattering sensor (LSS; Wetlabs Inc., USA), transmissometer (Wetlabs Inc.) and fluorometer (Chelsea, UK) was operated to collect hydrographic data along 500 m isobath. The CTD salinity values were calibrated against salinity values obtained from water samples collected simultaneously by a rosette sampler and analysed with a Guildline 8400 Autosol. Further, TRMM Microwave Imager (TMI) of Tropical Rainfall Measuring Mission (TRMM)-derived sea surface temperature (SST) and sea surface winds were used to examine spatial changes along

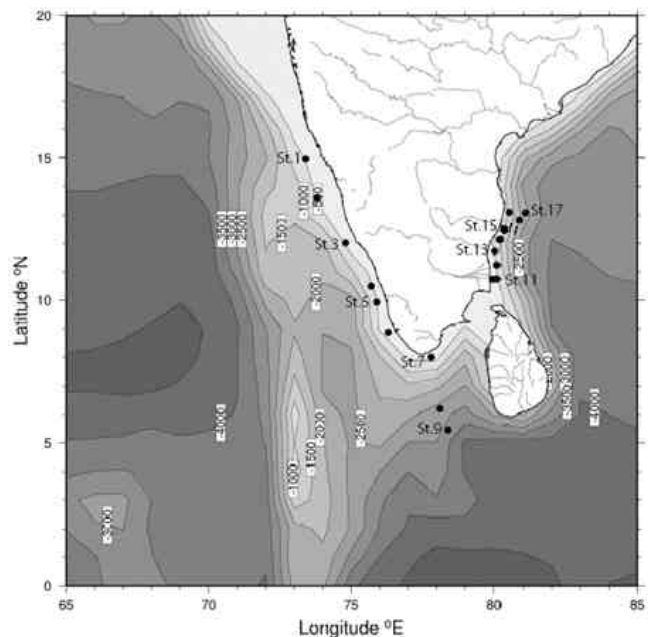


**Figure 1.** Study region with CTD locations.

\*For correspondence. (e-mail: anil@ncaor.org)

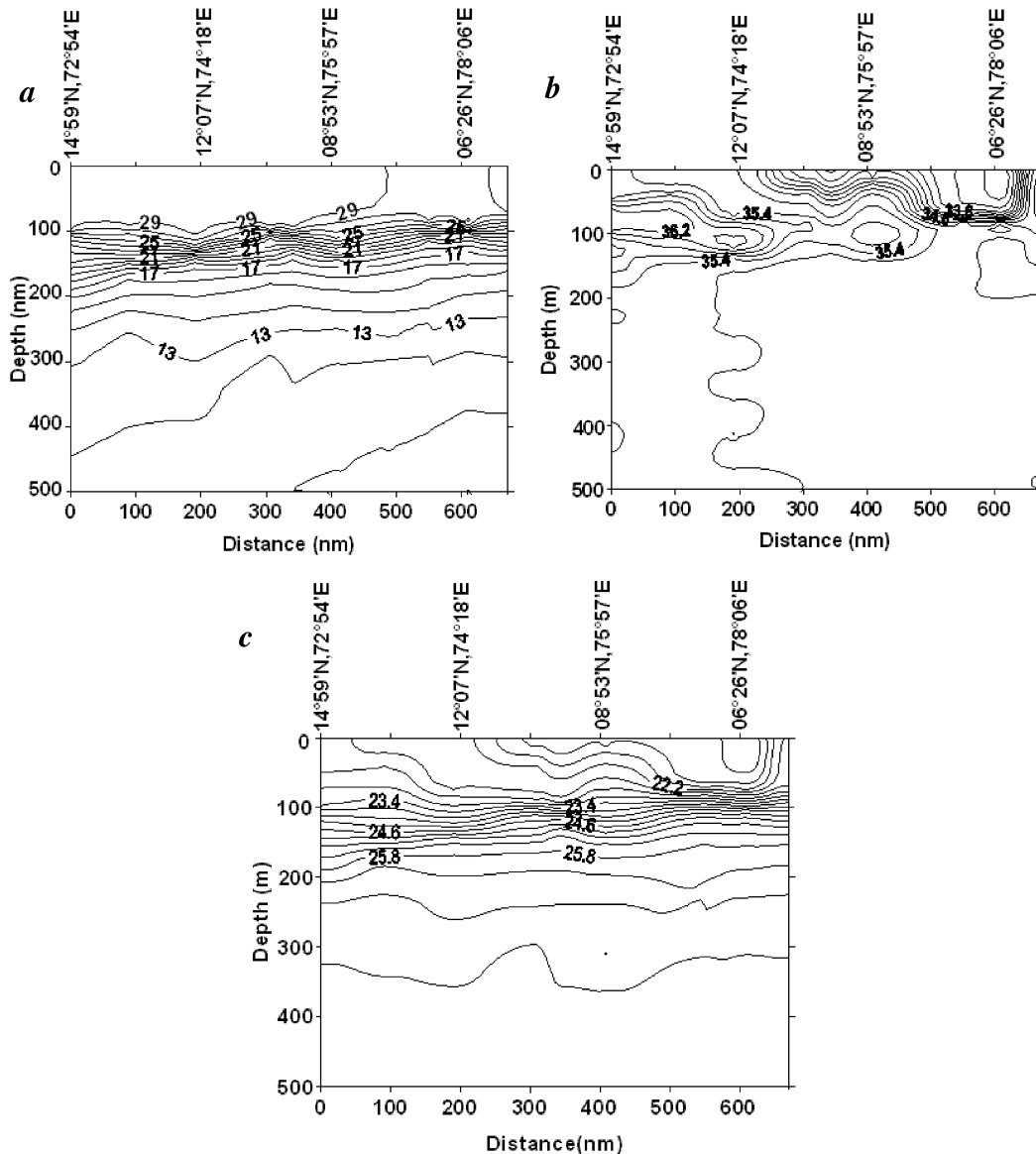


Figure 2. Vertical sections of (a) temperature (°C), (b) salinity (psu) and (c) density (kg m<sup>-3</sup>) along the southwest section.

the southwest and southeast transect during the period of the present *in situ* observations. Both the products are available at a spatial resolution of 0.25 × 0.25° latitude grid and downloaded from ftp.ssmi.com. The TMI provides wind speed at two microwave channels, namely 11 and 37 GHz. In the present study, we considered the winds measured at 11 GHz due to the surface transparency and consistency with the SST channel.

Vertical distribution of temperature, salinity and sigma-*t* as well as vertical profiles for LSS, transmissometer and fluorometer were prepared to examine the post-tsunami oceanographic conditions of southern Arabian Sea and the Bay of Bengal. The LSS and transmissometer data were collected from the region. Heat content along the southwest and southeast coasts was estimated with reference to the depth of 20°C isotherm (mid-thermocline depth). The heat content is estimated from the following equation:

$$H = rCp \left[ \int_0^z \bar{T} dz \right],$$

where *H* is the heat content (J m<sup>-2</sup>), *r* the density of sea water (kg m<sup>-3</sup>) and *Cp* the specific heat at constant pressure (J kg<sup>-1</sup>°C<sup>-1</sup>). *rCp* is assumed as a constant (0.409 × 10<sup>7</sup> J m<sup>-3</sup>°C<sup>-1</sup>) and  $\bar{T}$  is the depth averaged value of temperature.

Data are presented as two sections. First, the southwest transect covering measurements between 15 to 5°N along the west coast of India and the Gulf of Mannar. Secondly, the southeast transect covering measurements between 10 and 13°N along the east coast of India.

Figure 2a shows the vertical thermal structure along the southwest transect. A well-developed warm layer of >28.5°C in the upper 100 m is seen north of 9°N. A relatively

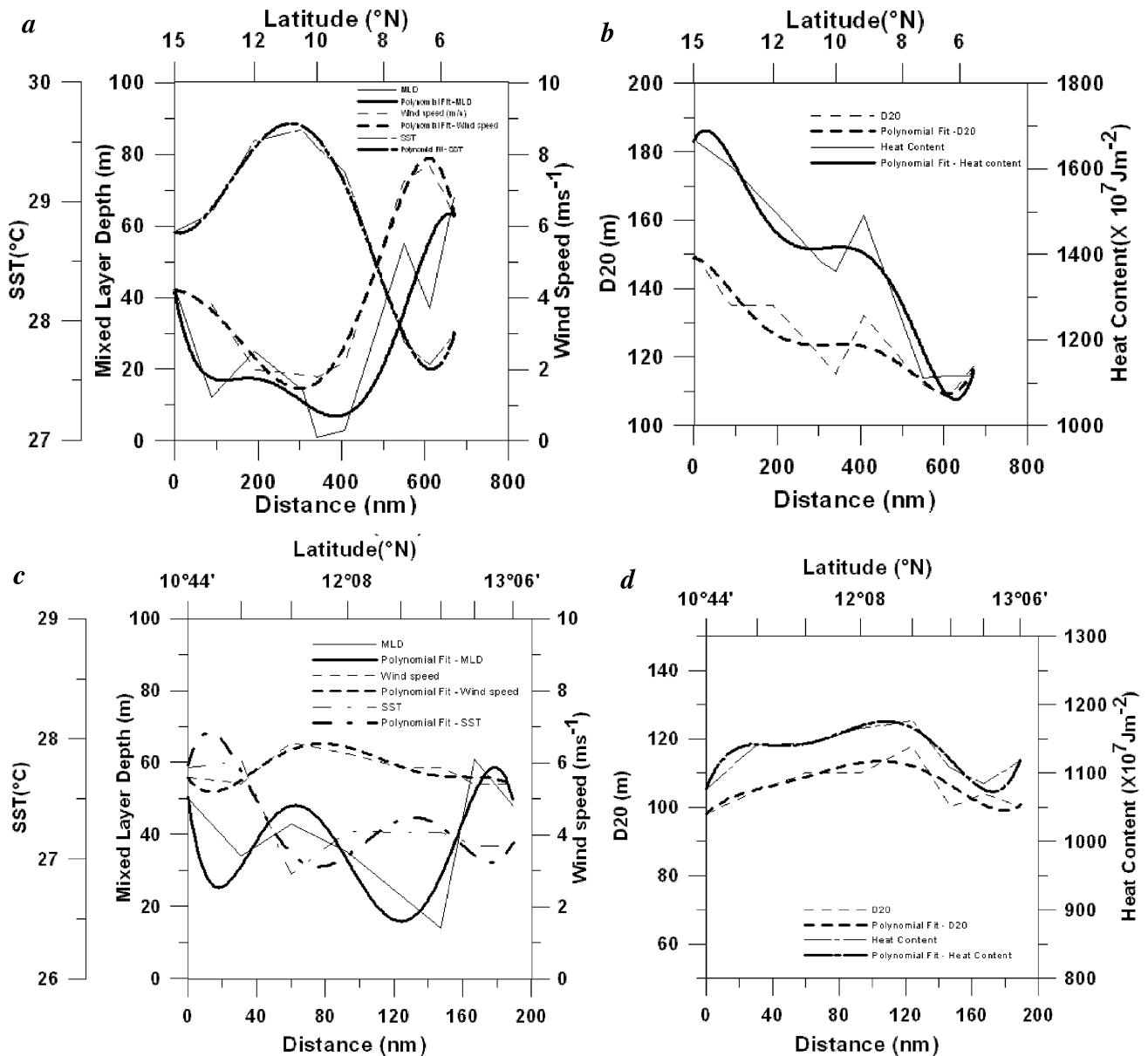


**Figure 3.** Distribution of (a) mixed layer depth, wind speed and sea surface temperature and (b) thermocline depth ( $D_{20}$ ) and heat content along southwest section, and (c) mixed layer depth, wind speed and sea surface temperature and (d) thermocline depth ( $D_{20}$ ) and heat content along southeast section.

cold-water region exists between 6 and 9°N. The thermocline is characterized by closely packed isotherm with larger thermal gradients in its upper portion. The penetration of high-salinity water (> 36 psu (practical salinity unit)) is visible in the upper 100 m in the northern regions of this section (Figure 2b). Though it subducts during its southward migration, the core of this high-salinity water mass remains around 100 m depth. This high-salinity water mass was earlier identified as Arabian Sea High Salinity Water mass (ASHSW), which forms in the northern Arabian Sea during winter<sup>12</sup>. A pool of low-salinity waters occupies the upper 50 m around 12°N. In the southern region of this transect where the surface salinity is low, the water den-

sity appears to follow the pattern of salinity distribution. However, below this shallow surface layer, the density follows the pattern of temperature (Figure 2c). The low-salinity waters observed along this section between 9 and 12°N are apparently from the Bay of Bengal, driven along the coast in to the Arabian Sea by coastally trapped currents<sup>9</sup>. During winter (November–February) both the westward-flowing north equatorial current between equator and 10°N, and the southward-flowing east India coastal current (EICC) bring warm and low-salinity waters into the Arabian Sea from the Bay of Bengal<sup>13</sup>.

The mixed layer depth (MLD), calculated using the density criterion<sup>14</sup>, along this transect showed a large variation

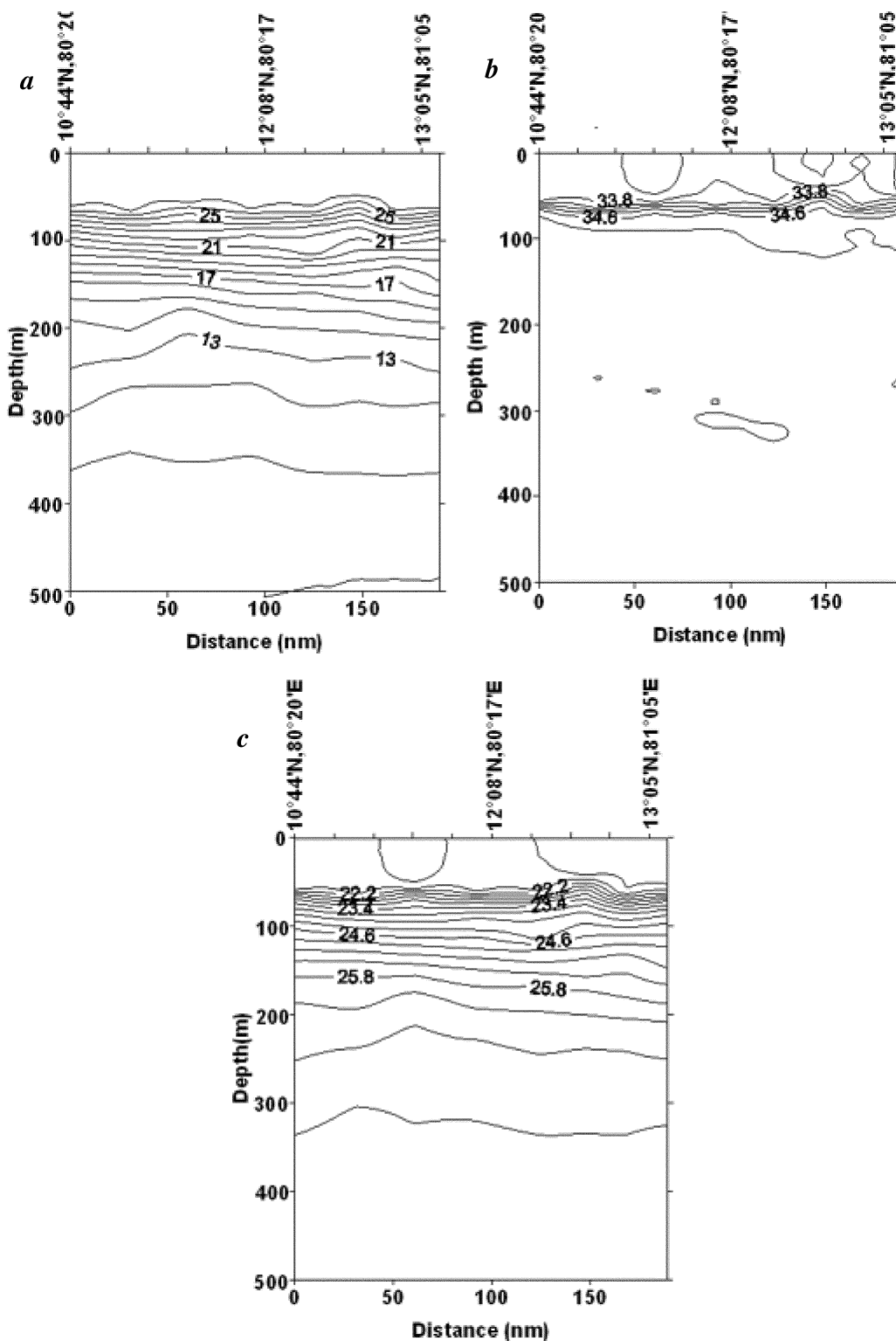


**Figure 4.** Vertical sections of (a) temperature (°C), (b) salinity (psu) and (c) density ( $\text{kg m}^{-3}$ ) along the southeast section (sts 16 and 17 are deep stations > 2500 m).

with greater than 50 m at 15°N that shoaled gradually to less than 3 m at 10°N (Figure 3a) and then rapidly increased southwards to 68 m at 5°46'N. Variation in wind speed along the coast also followed similar trend with moderate

to low winds ( $4\text{--}2 \text{ m s}^{-1}$ ) up to 10°N and rapidly strengthening to  $8 \text{ m s}^{-1}$  in the southernmost region of this transect. The measured SST showed an inverse trend with both winds and the MLD. The highest SST ( $29.6^\circ\text{C}$ ) around

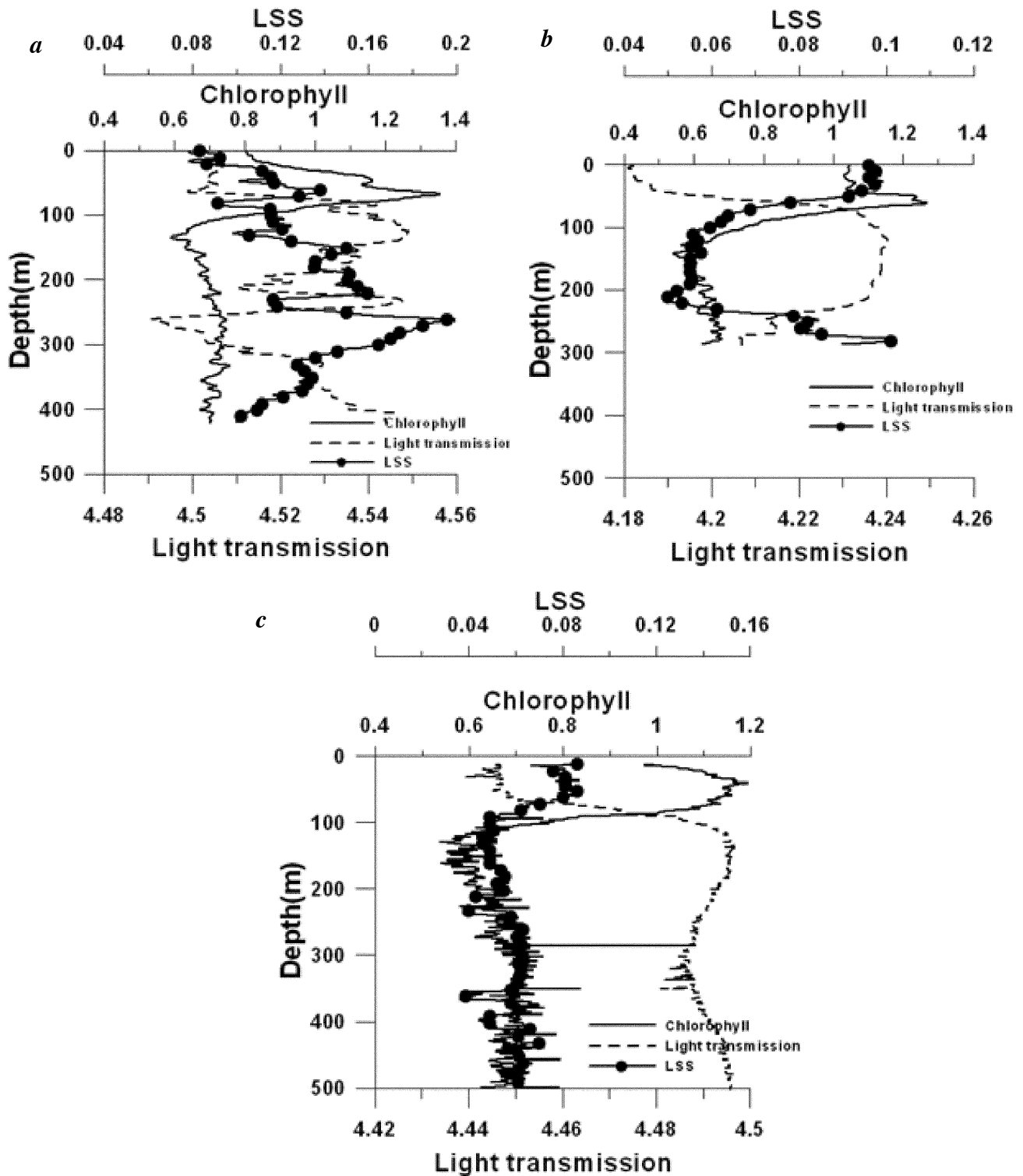


**Figure 5.** Vertical profiles of LSS ( $\text{mg l}^{-1}$ ), light transmission (V) and chlorophyll ( $\text{mg m}^{-3}$ ) along (a) st. 5, (b) st. 11 and (c) st. 9.

10°N was associated with the lowest MLD (3 m) and the lowest wind speed ( $1.84 \text{ m s}^{-1}$ ) observed along this transect. On the contrary, the lowest SST ( $27.6^\circ\text{C}$ ) around 6°N was associated with deep MLD (68 m) and relatively high wind speed ( $8 \text{ m s}^{-1}$ ). The north-south variation of thermocline

( $D_{20}$ ) and heat content with the polynomial fit showed that the thermocline depth varied from 150 m at 15°N to 117 m at 6°N. Heat content variability also showed a similar pattern as that of thermocline depth (Figure 3 b). It decreased from 15 to 10°N by  $308 \times 10^7 \text{ J m}^{-2}$ . However, it increased

by  $132 \times 10^7 \text{ J m}^{-2}$  around  $9^\circ\text{N}$  and decreased further southwards rapidly. Decrease in the heat content in the south appears to be the result of entrainment cooling forced by thermocline upwelling in this region. We observed that the heat content of the water column up to  $D_{20}$  was high (low) in the northern (southern) region along this transect. This is in direct contrast with the findings of Luis and Kawamura<sup>15</sup>, who reported that along the southwest coast of India, the sea surface loses (gains) heat in the northern (southern) region. Upward tilting of (towards north) salinity contours noticed in our study along the west coast of India can be attributed to the advection of low-salinity Bay of Bengal water carried by northward-flowing west India coastal current<sup>9</sup>. This current is found to flow southward along the west coast of India during April–September and reverse northward during October–March due to an along-shore density gradient facilitated by the winter cooling in the northern Arabian Sea<sup>15</sup>.

The vertical distribution of temperature, salinity and density along the southeast transect, between Nagapattinam and Chennai are exhibited in Figure 4. The vertical thermal structure shows uniformly well-developed isothermal layer in the upper 50 m (Figure 4a). The thermocline shows a marginal slackening towards north with wavy isotherms between  $12$  and  $13^\circ\text{N}$ . A gentle downward tilt of the thermocline towards north with thermocline spreading north of  $12^\circ\text{N}$  is evident in the thermal structure. The vertical salinity structure shows the presence of a strong halocline around 60 m all along the transect (Figure 4b). The surface salinity is typical of the Bay of Bengal, with salinity values ranging from 33.0 to 33.7 psu. The freshwater discharged at the head of the Bay of Bengal during the southwest monsoon season flows southward along the coast by the coastal currents during winter period<sup>9</sup>. The relatively high saline waters (33.7 psu) are seen north of Nagapattinam, separating two low-salinity pockets in the upper 50 m between  $10^\circ44'$  and  $13^\circ06'\text{N}$ . The vertical density structure is identical with the vertical structure of temperature despite large variation in salinity in the upper 50 m (Figure 4c). A dome-like structure is seen around  $12^\circ45'\text{N}$  in the vertical structure of temperature, salinity and density associated with northward spreading of the isolines.

However, the aforesaid thermohaline structure along the southwest and southeast coasts does not indicate any remarkable changes compared to earlier findings<sup>9,13</sup> in the hydrographic conditions of the present study region which experienced the massive impact of the tsunami. Hence it can be suggested that the hydrographic conditions of both southwest and southeast coasts do not exhibit any major changes after 1–2 weeks of the devastating tsunami.

Figure 3c exhibits the north-south variation of MLD, wind speed and SST, together with a polynomial fit to the data along the southeast transect. The MLD was about 50 m at the southern region of this transect, but shoaled to  $< 15$  m north of Nagapattinam. Further northwards, it rapidly increased to about 60 m. Along this coast, the wind speed

was more or less uniform around  $4 \text{ m s}^{-1}$  up to Nagapattinam, but rapidly increased to  $8 \text{ m s}^{-1}$ .  $D_{20}$  and MLD exhibited mutually opposite trend. The heat content varied between 1077 and  $1165 \times 10^7 \text{ J m}^{-2}$  and portrayed the same trend of  $D_{20}$  (Figure 3d). The highest value of the heat content was associated with deepest thermocline depth and shallow MLD observed at station 15 ( $12^\circ29'\text{N}$ ,  $80^\circ40'\text{E}$ ).

During this survey, we have used three optical sensors, namely LSS, transmissometer and fluorometer to investigate the distribution of suspended matter in the water column that might have arisen due to the turbulence generated by the tsunami. The aforesaid observations were made up to 5 m above the ocean floor for shallow stations ( $\leq 500$  m), whereas for deep stations ( $\geq 1000$  m), measurements were restricted up to 500 m. Figure 5a to c shows typical vertical profiles of LSS ( $\text{mg l}^{-1}$ ) and light transmission (V) and chlorophyll ( $\text{mg m}^{-3}$ , as measured by the fluorometer) for coastal (sts. 5 and 11) and open waters (st. 9) respectively. Figure 5a shows a shallow layer of high LSS signal ( $0.14031 \text{ mg l}^{-1}$ ) between 20 and 60 m associated with high chlorophyll and low light transmission. This layer of high-scattering obviously indicates the subsurface chlorophyll maximum which is known to exist in this region during this period<sup>16</sup>. Below 230 m depth, a broad high-scattering layer appears ( $0.199185 \text{ mg l}^{-1}$ ), which is not associated with bioproductivity as seen from the chlorophyll profile. As this station is in shallow waters, we presume that the high-scattering at this depth is caused by particles brought into suspension from the sea-floor sediments due to turbulent interaction generated by the tsunami. Similar feature can be seen off Nagapattinam (st. 11), where the high-scattering layer ( $0.1021 \text{ mg l}^{-1}$ ) appears below 210 m (Figure 5b). The open ocean profiles at station 9 (Figure 5c) show a single shallow high-scattering layer associated with subsurface chlorophyll maximum between 20 and 60 m depth. This station represents a typical distribution of light scattering, transmission and chlorophyll expected in the oceans. Hence the high scattering at depth greater than 200 m, depending on the ocean depth, indicates layers of high turbidity (suspended matter) forced by turbulent interaction with sea-floor sediments due to the impact of tsunami in the coastal waters of India.

The tsunami appears to have influenced the coastal waters as evident from deep turbid layers near the coastal regions in southern Bay of Bengal. Thermohaline structure at deep stations is relatively unaffected by the tsunami, whereas the low-salinity waters concentrated in the southern Gulf of Mannar region along the southwest transect are carried by the EICC from the Bay of Bengal. Although the thermohaline structure appears to be typical of the winter season with low-salinity Bay of Bengal waters along the Kerala coast and the ASHSW around 100 m depth in the southwest section, the thermohaline structure along the southeast transect shows uncharacteristically cold ( $< 27^\circ\text{C}$ ) and fairly well-developed MLD. A marginal downward tilt of thermocline towards north can be observed

in the southeast coast. The deep turbid layers observed near the coast are attributed to resuspension of the bottom sediments due to the tsunami. The present study however calls for a long-term monitoring of the ecosystem changes caused by the tsunami near the affected coast.

## Molecular characterization of *Trichoderma* taxa causing green mould disease in edible mushrooms

S. K. Singh\*, V. P. Sharma, S. R. Sharma, Satish Kumar and Mugdha Tiwari

National Research Centre for Mushroom (ICAR), Chambaghat, Solan 173 213, India

***Trichoderma* taxa associated with green mould disorder of edible mushrooms were isolated from both fruit bodies and substrates of *Agaricus bisporus*, *A. bitorquis*, *Calocybe indica*, *Ganoderma lucidum*, *Lentinula edodes*, *Pleurotus sajor-caju*, and *Volvariella volvacea*. Emerged fruiting bodies in the affected portion of the substrate were badly spotted, brownish in colour and reduced in both growth rate and yield performance. Microscopic examination of cultures revealed significant differences in fungal morphology, but were difficult to designate as *Trichoderma* species. The nucleotide sequence comparisons of 5.8S rRNA gene using BLAST network facilitated molecular identification and genetic cataloguing of 18 *Trichoderma* isolates into two taxa, namely *T. harzianum* and *T. virens*. RAPD primers exhibited both inter- and intra-specific variations among the test isolates and separated them into eight distinct phylogenetic sub-clades. The present study underlines the potential threat of green mould disorders in cultivated mushrooms and validates existence of significant intraspecific diversity in isolates of both *T. harzianum* and *T. virens*.**

**Keywords:** Edible mushrooms, green mould disease, molecular identification, *Trichoderma*.

MUSHROOM cultivation is a controlled biological system, which depends upon many biotic and abiotic factors, and contamination by several microorganisms during cultivation is manifested. Among the biotic factors, fungi both parasitic and competitor, are the most important group which are generally encountered during cultivation of mushrooms. *Trichoderma* species causing green mould is one of the most serious problems in the mushroom industry globally. Sinden and Houser<sup>1</sup> were the first to recognize *Trichoderma* species as a potentially important pathogen and/or competitor that may effect the production of white button mushroom. *Trichoderma* outbreaks have led to a total loss of mushroom production in many commercial mushroom farms<sup>2</sup>. Different levels of crop losses ranging from 10 to 80% have been reported from various parts of the world<sup>3-6</sup>. Serious crop losses due to *Trichoderma* species have not only been reported in *Agaricus bisporus* but also in other commercially cultivated edible mushrooms<sup>7-10</sup>.

*Trichoderma* species grow rapidly in versatile conditions and utilize various kinds of substrates<sup>11</sup>. Different species

1. Banse, K., On upwelling and bottom-trawling off the south west coast of India. *J. Mar. Biol. Assoc. India*, 1959, **1**, 33-49.
2. Brock, J. C., McClaim, C. R. and Hay, W. W., A south-west monsoon hydrographic climatology for the northern Arabian Sea. *J. Geophys. Res.*, 1992, **97**, 9455-9465.
3. Darbyshire, M., The surface waters off the coast of Kerala, south-west India. *Deep Sea Res.*, 1967, **14**, 295-320.
4. Jayaraman, R., Ramamirtham, C. P., Sundaram, K. V. and Aravindakshan Nair, C. P., Hydrography of the Laccadive offshore waters. *J. Mar. Biol. Assoc. India*, 1960, **2**, 24-34.
5. La Fond, E. C., Oceanographic studies in the Bay of Bengal. *Proc. Indian Acad. Sci. (Earth Planet. Sci.)*, 1957, **46**, 1-46.
6. Muraleedharan, P. M. and Kumar, S. P., Arabian Sea upwelling – A comparison between coastal and open ocean regions. *Curr. Sci.*, 1996, **71**, 824-846.
7. Patil, M. R. and Ramamirtham, C. P., Hydrography of the Laccadive offshore waters – A study of winter conditions. *J. Mar. Biol. Assoc. India*, 1963, **5**, 159-169.
8. Sastry, A. A. and Myrland, P., Distribution of temperature, salinity and density in the Arabian Sea along the south Malabar coast (south India) during the post-monsoon season. *Indian J. Fish.*, 1959, **6**, 223-255.
9. Shetye, S. R., Gouveia, A. D., Shenoi, S. S. C., Sundar, D., Michael, G. S., Almedia, A. M. and Santanam, K., The coastal current off western India during the northeast monsoon. *Deep Sea Res.*, 1991, **38**, 1517-1529.
10. Sharma, G. S., Upwelling off the southwest coast of India. *Indian J. Mar. Sci.*, 1978, **7**, 209-218.
11. Vardachari, V. V. R., Murty, C. S. and Sankaranarayanan, V. N., Physical characteristics of waters and water masses off the west coast of India during late spring. *Indian J. Mar. Sci.*, 1974, **3**, 1-3.
12. Prasanna Kumar, S. and Prasad, T. G., Winter cooling in the northern Arabian sea. *Curr. Sci.*, 1996, **71**, 834-841.
13. Prasanna Kumar, S. *et al.*, Intrusion of the Bay of Bengal water into the Arabian Sea during winter monsoon and associated chemical and biological response. *Geophys. Res. Lett.*, 2004, **31**, L15304, doi:10.1029/2004GL020247.
14. Thompson, R. E. and Fine, I. V., Estimating mixed layer depth from oceanic profile data. *J. Atmos. Oceanogr. Technol.*, 2003, **20**, 319-329.
15. Luis, A. J. and Kawamura, H., Seasonal SST patterns along the west India shelf inferred from AVHRR. *Remote Sensing Environ.*, 2003, **86**, 2006-2015.
16. Bhattathiri, P. M. A., Aditi Pant, Sureka Sawant, Gauns. M., Mathondkar, S. G. P. and Mohanraju, M., Phytoplankton production and chlorophyll distribution in the eastern and central Arabian Sea. *Curr. Sci.*, 1996, **71**, 857-862.

**ACKNOWLEDGEMENTS.** We thank the Secretary, Department of Ocean Development, New Delhi for successful planning and execution of this post-tsunami expedition, and the help provided for making the research ship available for this study to acquire relevant datasets.

Received 6 April 2005; revised accepted 28 December 2005

\*For correspondence. (e-mail: sksingh1111@hotmail.com)